

Study of the light scalar $a_0(980)$ through the decay $D^0 \rightarrow a_0(980)^- e^+ \nu_e$ with $a_0(980)^- \rightarrow \eta \pi^-$

- M. Ablikim¹, M. N. Achasov^{4,c}, P. Adlarson⁷⁶, O. Afedulidis³, X. C. Ai⁸¹, R. Aliberti³⁵, A. Amoroso^{75A,75C}, Q. An^{72,58,a}, Y. Bai⁵⁷, O. Bakina³⁶, I. Balossino^{29A}, Y. Ban^{46,h}, H.-R. Bao⁶⁴, V. Batozskaya^{1,44}, K. Begzsuren³², N. Berger³⁵, M. Berlowski⁴⁴, M. Bertani^{28A}, D. Bettoni^{29A}, F. Bianchi^{75A,75C}, E. Bianco^{75A,75C}, A. Bortone^{75A,75C}, I. Boyko³⁶, R. A. Briere⁵, A. Brueggemann⁶⁹, H. Cai⁷⁷, X. Cai^{1,58}, A. Calcaterra^{28A}, G. F. Cao^{1,64}, N. Cao^{1,64}, S. A. Cetin^{62A}, X. Y. Chai^{46,h}, J. F. Chang^{1,58}, G. R. Che⁴³, Y. Z. Che^{1,58,64}, G. Chelkov^{36,b}, C. Chen⁴³, C. H. Chen⁹, Chao Chen⁵⁵, G. Chen¹, H. S. Chen^{1,64}, H. Y. Chen²⁰, M. L. Chen^{1,58,64}, S. J. Chen⁴², S. L. Chen⁴⁵, S. M. Chen⁶¹, T. Chen^{1,64}, X. R. Chen^{31,64}, X. T. Chen^{1,64}, Y. B. Chen^{1,58}, Y. Q. Chen³⁴, Z. J. Chen^{25,i}, Z. Y. Chen^{1,64}, S. K. Choi¹⁰, G. Cibinetto^{29A}, F. Cossio^{75C}, J. J. Cui⁵⁰, H. L. Dai^{1,58}, J. P. Dai⁷⁹, A. Dbeysi¹⁸, R. E. de Boer³, D. Dedovich³⁶, C. Q. Deng⁷³, Z. Y. Deng¹, A. Denig³⁵, I. Denysenko³⁶, M. Destefanis^{75A,75C}, F. De Mori^{75A,75C}, B. Ding^{67,1}, X. X. Ding^{46,h}, Y. Ding⁴⁰, Y. Ding³⁴, J. Dong^{1,58}, L. Y. Dong^{1,64}, M. Y. Dong^{1,58,64}, X. Dong⁷⁷, M. C. Du¹, S. X. Du⁸¹, Y. Y. Duan⁵⁵, Z. H. Duan⁴², P. Egorov^{36,b}, Y. H. Fan⁴⁵, J. Fang⁵⁰, J. Fang^{1,58}, S. S. Fang^{1,64}, W. X. Fang¹, Y. Fang¹, Y. Q. Fang^{1,58}, R. Farinelli^{29A}, L. Fava^{75B,75C}, F. Feldbauer³, G. Felici^{28A}, C. Q. Feng^{72,58}, J. H. Feng⁵⁹, Y. T. Feng^{72,58}, M. Fritsch³, C. D. Fu¹, J. L. Fu⁶⁴, Y. W. Fu^{1,64}, H. Gao⁶⁴, X. B. Gao⁴¹, Y. N. Gao^{46,h}, Yang Gao^{72,58}, S. Garbolino^{75C}, I. Garzia^{29A,29B}, L. Ge⁸¹, P. T. Ge¹⁹, Z. W. Ge⁴², C. Geng⁵⁹, E. M. Gersabeck⁶⁸, A. Gilman⁷⁰, K. Goetzen¹³, L. Gong⁴⁰, W. X. Gong^{1,58}, W. Gradl³⁵, S. Gramigna^{29A,29B}, M. Greco^{75A,75C}, M. H. Gu^{1,58}, Y. T. Gu¹⁵, C. Y. Guan^{1,64}, A. Q. Guo^{31,64}, L. B. Guo⁴¹, M. J. Guo⁵⁰, R. P. Guo⁴⁹, Y. P. Guo^{12,g}, A. Guskov^{36,b}, J. Gutierrez²⁷, K. L. Han⁶⁴, T. T. Han¹, F. Hanisch³, X. Q. Hao¹⁹, F. A. Harris⁶⁶, K. K. He⁵⁵, K. L. He^{1,64}, F. H. Heinsius³, C. H. Heinz³⁵, Y. K. Heng^{1,58,64}, C. Herold⁶⁰, T. Holtmann³, P. C. Hong³⁴, G. Y. Hou^{1,64}, X. T. Hou^{1,64}, Y. R. Hou⁶⁴, Z. L. Hou¹, B. Y. Hu⁵⁹, H. M. Hu^{1,64}, J. F. Hu^{56,j}, Q. P. Hu^{72,58}, S. L. Hu^{12,g}, T. Hu^{1,58,64}, Y. Hu¹, G. S. Huang^{72,58}, K. X. Huang⁵⁹, L. Q. Huang^{31,64}, X. T. Huang⁵⁰, Y. P. Huang¹, Y. S. Huang⁵⁹, T. Hussain⁷⁴, F. Hölzken³, N. Hüskens³⁵, N. in der Wiesche⁶⁹, J. Jackson²⁷, S. Janchiv³², J. H. Jeong¹⁰, Q. Ji¹, Q. P. Ji¹⁹, W. Ji^{1,64}, X. B. Ji^{1,64}, X. L. Ji^{1,58}, Y. Y. Ji⁵⁰, X. Q. Jia⁵⁰, Z. K. Jia^{72,58}, D. Jiang^{1,64}, H. B. Jiang⁷⁷, P. C. Jiang^{46,h}, S. S. Jiang³⁹, T. J. Jiang¹⁶, X. S. Jiang^{1,58,64}, Y. Jiang⁶⁴, J. B. Jiao⁵⁰, J. K. Jiao³⁴, Z. Jiao²³, S. Jin⁴², Y. Jin⁶⁷, M. Q. Jing^{1,64}, X. M. Jing⁶⁴, T. Johansson⁷⁶, S. Kabana³³, N. Kalantar-Nayestanaki⁶⁵, X. L. Kang⁹, X. S. Kang⁴⁰, M. Kavatsyuk⁶⁵, B. C. Ke⁸¹, V. Khachatryan²⁷, A. Khoukaz⁶⁹, R. Kiuchi¹, O. B. Kolcu^{62A}, B. Kopf³, M. Kuessner³, X. Kui^{1,64}, N. Kumar²⁶, A. Kupsc^{44,76}, W. Kühn³⁷, L. Lavezzi^{75A,75C}, T. T. Lei^{72,58}, Z. H. Lei^{72,58}, M. Lellmann³⁵, T. Lenz³⁵, C. Li⁴⁷, C. Li⁴³, C. H. Li³⁹, Cheng Li^{72,58}, D. M. Li⁸¹, F. Li^{1,58}, G. Li¹, H. B. Li^{1,64}, H. J. Li¹⁹, H. N. Li^{56,j}, Hui Li⁴³, J. R. Li⁶¹, J. S. Li⁵⁹, K. Li¹, K. L. Li¹⁹, L. J. Li^{1,64}, L. K. Li¹, Lei Li⁴⁸, M. H. Li⁴³, P. R. Li^{38,k,l}, Q. M. Li^{1,64}, Q. X. Li⁵⁰, R. Li^{17,31}, S. X. Li¹², T. Li⁵⁰, W. D. Li^{1,64}, W. G. Li^{1,a}, X. Li^{1,64}, X. H. Li^{72,58}, X. L. Li⁵⁰, X. Y. Li^{1,64}, X. Z. Li⁵⁹, Y. G. Li^{46,h}, Z. J. Li⁵⁹, Z. Y. Li⁷⁹, C. Liang⁴², H. Liang^{1,64}, H. Liang^{72,58}, Y. F. Liang⁵⁴, Y. T. Liang^{31,64}, G. R. Liao¹⁴, Y. P. Liao^{1,64}, J. Libby²⁶, A. Limphirat⁶⁰, C. C. Lin⁵⁵, C. X. Lin⁶⁴, D. X. Lin^{31,64}, T. Lin¹, B. J. Liu¹, B. X. Liu⁷⁷, C. Liu³⁴, C. X. Liu¹, F. Liu¹, F. H. Liu⁵³, Feng Liu⁶, G. M. Liu^{56,j}, H. Liu^{38,k,l}, H. B. Liu¹⁵, H. H. Liu¹, H. M. Liu^{1,64}, Huihui Liu²¹, J. B. Liu^{72,58}, J. Y. Liu^{1,64}, K. Liu^{38,k,l}, K. Y. Liu⁴⁰, Ke Liu²², L. Liu^{72,58}, L. C. Liu⁴³, Lu Liu⁴³, M. H. Liu^{12,g}, P. L. Liu¹, Q. Liu⁶⁴, S. B. Liu^{72,58}, T. Liu^{12,g}, W. K. Liu⁴³, W. M. Liu^{72,58}, X. Liu³⁹, X. Liu^{38,k,l}, Y. Liu⁸¹, Y. Liu^{38,k,l}, Y. B. Liu⁴³, Z. A. Liu^{1,58,64}, Z. D. Liu⁹, Z. Q. Liu⁵⁰, X. C. Lou^{1,58,64}, F. X. Lu⁵⁹, H. J. Lu²³, J. G. Lu^{1,58}, X. L. Lu¹, Y. Lu⁷, Y. P. Lu^{1,58}, Z. H. Lu^{1,64}, C. L. Luo⁴¹, J. R. Luo⁵⁹, M. X. Luo⁸⁰, T. Luo^{12,g}, X. L. Luo^{1,58}, X. R. Lyu⁶⁴, Y. F. Lyu⁴³, F. C. Ma⁴⁰, H. Ma⁷⁹, H. L. Ma¹, J. L. Ma^{1,64}, L. L. Ma⁵⁰, L. R. Ma⁶⁷, M. M. Ma^{1,64}, Q. M. Ma¹, R. Q. Ma^{1,64}, T. Ma^{72,58}, X. T. Ma^{1,64}, X. Y. Ma^{1,58}, Y. M. Ma³¹, F. E. Maas¹⁸, I. MacKay⁷⁰, M. Maggiora^{75A,75C}, S. Malde⁷⁰, Y. J. Mao^{46,h}, Z. P. Mao¹, S. Marcello^{75A,75C}, Z. X. Meng⁶⁷, J. G. Messchendorp^{13,65}, G. Mezzadri^{29A}, H. Miao^{1,64}, T. J. Min⁴², R. E. Mitchell²⁷, X. H. Mo^{1,58,64}, B. Moses²⁷, N. Yu. Muchnoi^{4,c}, J. Muskalla³⁵, Y. Nefedov³⁶, F. Nerling^{18,e}, L. S. Nie²⁰, I. B. Nikolaev^{4,c}, Z. Ning^{1,58}, S. Nisan^{11,m}, Q. L. Niu^{38,k,l}, W. D. Niu⁵⁵, Y. Niu⁵⁰, S. L. Olsen^{10,64}, S. L. Olsen⁶⁴, Q. Ouyang^{1,58,64}, S. Pacetti^{28B,28C}, X. Pan⁵⁵, Y. Pan⁵⁷, A. Pathak³⁴, Y. P. Pei^{72,58}, M. Pelizaeus³, H. P. Peng^{72,58}, Y. Y. Peng^{38,k,l}, K. Peters^{13,e}, J. L. Ping⁴¹, R. G. Ping^{1,64}, S. Plura³⁵, V. Prasad³³, F. Z. Qi¹, H. Qi^{72,58}, H. R. Qi⁶¹, M. Qi⁴², T. Y. Qi^{12,g}, S. Qian^{1,58}, W. B. Qian⁶⁴, C. F. Qiao⁶⁴, X. K. Qiao⁸¹, J. J. Qin⁷³, L. Q. Qin¹⁴, L. Y. Qin^{72,58}, X. P. Qin^{12,g}, X. S. Qin⁵⁰, Z. H. Qin^{1,58}, J. F. Qiu¹, Z. H. Qu⁷³, C. F. Redmer³⁵, K. J. Ren³⁹, A. Rivetti^{75C}, M. Roloff^{75C}, G. Rong^{1,64}, Ch. Rosner¹⁸, M. Q. Ruan^{1,58}, S. N. Ruan⁴³, N. Salone⁴⁴, A. Sarantsev^{36,d}, Y. Schelhaas³⁵, K. Schoenning⁷⁶, M. Scoglio^{29A}, K. Y. Shan^{12,g}, W. Shan²⁴, X. Y. Shan^{72,58}, Z. J. Shang^{38,k,l}, J. F. Shangguan¹⁶, L. G. Shao^{1,64}, M. Shao^{72,58}, C. P. Shen^{12,g}, H. F. Shen^{1,8}, W. H. Shen⁶⁴, X. Y. Shen^{1,64}, B. A. Shi⁶⁴, H. Shi^{72,58}, H. C. Shi^{72,58}, J. L. Shi^{12,g}, J. Y. Shi¹, Q. Q. Shi⁵⁵, S. Y. Shi⁷³, X. Shi^{1,58}, J. J. Song¹⁹, T. Z. Song⁵⁹, W. M. Song^{34,1}, Y. J. Song^{12,g}, Y. X. Song^{46,h,n}, S. Sosio^{75A,75C}, S. Spataro^{75A,75C}, F. Stieler³⁵, S. S. Su⁴⁰, Y. J. Su⁶⁴, G. B. Sun⁷⁷, G. X. Sun¹, H. Sun⁶⁴, H. K. Sun¹, J. F. Sun¹⁹, K. Sun⁶¹, L. Sun⁷⁷, S. S. Sun^{1,64}, T. Sun^{51,f}, W. Y. Sun³⁴, Y. Sun⁹, Y. J. Sun^{72,58}, Y. Z. Sun¹, Z. Q. Sun^{1,64}, Z. T. Sun⁵⁰, C. J. Tang⁵⁴, G. Y. Tang¹, J. Tang⁵⁹, M. Tang^{72,58}, Y. A. Tang⁷⁷, L. Y. Tao⁷³, Q. T. Tao^{25,i}, M. Tat⁷⁰, J. X. Teng^{72,58}, V. Thoren⁷⁶, W. H. Tian⁵⁹, Y. Tian^{31,64}, Z. F. Tian⁷⁷, I. Uman^{62B}, Y. Wan⁵⁵, S. J. Wang⁵⁰, B. Wang¹, B. L. Wang⁶⁴, Bo Wang^{72,58}, D. Y. Wang^{46,h}, F. Wang⁷³, H. J. Wang^{38,k,l}, J. J. Wang⁷⁷, J. P. Wang⁵⁰, K. Wang^{1,58}, L. L. Wang¹, M. Wang⁵⁰, N. Y. Wang⁶⁴, S. Wang^{12,g}, S. Wang^{38,k,l}, T. Wang^{12,g}, T. J. Wang⁴³, W. Wang⁵⁹, W. Wang⁷³, W. P. Wang^{35,58,72,o}, X. Wang^{46,h}, X. F. Wang^{38,k,l}, X. J. Wang³⁹, X. L. Wang^{12,g}, X. N. Wang¹, Y. Wang⁶¹, Y. D. Wang⁴⁵, Y. F. Wang^{1,58,64}, Y. H. Wang^{38,k,l}, Y. L. Wang¹⁹, Y. N. Wang⁴⁵, Y. Q. Wang¹, Yaqian Wang¹⁷, Yi Wang⁶¹, Z. Wang^{1,58}, Z. L. Wang⁷³, Z. Y. Wang^{1,64}, Ziyi Wang⁶⁴, D. H. Wei¹⁴, F. Weidner⁶⁹, S. P. Wen¹, Y. R. Wen³⁹, U. Wiedner³, G. Wilkinson⁷⁰, M. Wolke⁷⁶, L. Wollenberg³, C. Wu³⁹, J. F. Wu^{1,8}, L. H. Wu^{1,64}, X. Wu^{12,g}, X. H. Wu³⁴, Y. Wu^{72,58}, Y. H. Wu⁵⁵, Y. J. Wu³¹, Z. Wu^{1,58}, L. Xia^{72,58}, X. M. Xian³⁹, B. H. Xiang^{1,64}, T. Xiang^{46,h}, D. Xiao^{38,k,l}, G. Y. Xiao⁴², S. Y. Xiao¹, Y. L. Xiao^{12,g}, Z. J. Xiao⁴¹, C. Xie⁴², X. H. Xie^{46,h}, Y. Xie⁵⁰, Y. G. Xie^{1,58}, Y. H. Xie⁶,

Z. P. Xie^{72,58}, T. Y. Xing^{1,64}, C. F. Xu^{1,64}, C. J. Xu⁵⁹, G. F. Xu¹, H. Y. Xu^{67,2}, M. Xu^{72,58}, Q. J. Xu¹⁶, Q. N. Xu³⁰, W. Xu¹, W. L. Xu⁶⁷, X. P. Xu⁵⁵, Y. Xu⁴⁰, Y. C. Xu⁷⁸, Z. S. Xu⁶⁴, F. Yan^{12,g}, L. Yan^{12,g}, W. B. Yan^{72,58}, W. C. Yan⁸¹, X. Q. Yan^{1,64}, H. J. Yang^{51,f}, H. L. Yang³⁴, H. X. Yang¹, J. H. Yang⁴², T. Yang¹, Y. Yang^{12,g}, Y. F. Yang⁴³, Y. F. Yang^{1,64}, Y. X. Yang^{1,64}, Z. W. Yang^{38,k,l}, Z. P. Yao⁵⁰, M. Ye^{1,58}, M. H. Ye⁸, J. H. Yin¹, Junhao Yin⁴³, Z. Y. You⁵⁹, B. X. Yu^{1,58,64}, C. X. Yu⁴³, G. Yu^{1,64}, J. S. Yu^{25,i}, M. C. Yu⁴⁰, T. Yu⁷³, X. D. Yu^{46,h}, Y. C. Yu⁸¹, C. Z. Yuan^{1,64}, J. Yuan⁴⁵, J. Yuan³⁴, L. Yuan², S. C. Yuan^{1,64}, Y. Yuan^{1,64}, Z. Y. Yuan⁵⁹, C. X. Yue³⁹, A. A. Zafar⁷⁴, F. R. Zeng⁵⁰, S. H. Zeng^{63A,63B,63C,63D}, X. Zeng^{12,g}, Y. Zeng^{25,i}, Y. J. Zeng^{1,64}, Y. J. Zeng⁵⁹, X. Y. Zhai³⁴, Y. C. Zhai⁵⁰, Y. H. Zhan⁵⁹, A. Q. Zhang^{1,64}, B. L. Zhang^{1,64}, B. X. Zhang¹, D. H. Zhang⁴³, G. Y. Zhang¹⁹, H. Zhang^{72,58}, H. Zhang⁸¹, H. C. Zhang^{1,58,64}, H. H. Zhang⁵⁹, H. H. Zhang³⁴, H. Q. Zhang^{1,58,64}, H. R. Zhang^{72,58}, H. Y. Zhang^{1,58}, J. Zhang⁸¹, J. Zhang⁵⁹, J. J. Zhang⁵², J. L. Zhang²⁰, J. Q. Zhang⁴¹, J. S. Zhang^{12,g}, J. W. Zhang^{1,58,64}, J. X. Zhang^{38,k,l}, J. Y. Zhang¹, J. Z. Zhang^{1,64}, Jianyu Zhang⁶⁴, L. M. Zhang⁶¹, Lei Zhang⁴², P. Zhang^{1,64}, Q. Y. Zhang³⁴, R. Y. Zhang^{38,k,l}, S. H. Zhang^{1,64}, Shulei Zhang^{25,i}, X. M. Zhang¹, X. Y. Zhang⁴⁰, X. Y. Zhang⁵⁰, Y. Zhang¹, Y. Zhang⁷³, Y. T. Zhang⁸¹, Y. H. Zhang^{1,58}, Y. M. Zhang³⁹, Yan Zhang^{72,58}, Z. D. Zhang¹, Z. H. Zhang¹, Z. L. Zhang³⁴, Z. Y. Zhang⁴³, Z. Y. Zhang⁷⁷, Z. Z. Zhang⁴⁵, G. Zhao¹, J. Y. Zhao^{1,64}, J. Z. Zhao^{1,58}, L. Zhao¹, Lei Zhao^{72,58}, M. G. Zhao⁴³, N. Zhao⁷⁹, R. P. Zhao⁶⁴, S. J. Zhao⁸¹, Y. B. Zhao^{1,58}, Y. X. Zhao^{31,64}, Z. G. Zhao^{72,58}, A. Zhemchugov^{36,b}, B. Zheng⁷³, B. M. Zheng³⁴, J. P. Zheng^{1,58}, W. J. Zheng^{1,64}, Y. H. Zheng⁶⁴, B. Zhong⁴¹, X. Zhong⁵⁹, H. Zhou⁵⁰, J. Y. Zhou³⁴, L. P. Zhou^{1,64}, S. Zhou⁶, X. Zhou⁷⁷, X. K. Zhou⁶, X. R. Zhou^{72,58}, X. Y. Zhou³⁹, Y. Z. Zhou^{12,g}, Z. C. Zhou²⁰, A. N. Zhu⁶⁴, J. Zhu⁴³, K. Zhu¹, K. J. Zhu^{1,58,64}, K. S. Zhu^{12,g}, L. Zhu³⁴, L. X. Zhu⁶⁴, S. H. Zhu⁷¹, T. J. Zhu^{12,g}, W. D. Zhu⁴¹, Y. C. Zhu^{72,58}, Z. A. Zhu^{1,64}, J. H. Zou¹, J. Zu^{72,58}

(BESIII Collaboration)

¹ Institute of High Energy Physics, Beijing 100049, People's Republic of China

² Beihang University, Beijing 100191, People's Republic of China

³ Bochum Ruhr-University, D-44780 Bochum, Germany

⁴ Budker Institute of Nuclear Physics SB RAS (BINP), Novosibirsk 630090, Russia

⁵ Carnegie Mellon University, Pittsburgh, Pennsylvania 15213, USA

⁶ Central China Normal University, Wuhan 430079, People's Republic of China

⁷ Central South University, Changsha 410083, People's Republic of China

⁸ China Center of Advanced Science and Technology, Beijing 100190, People's Republic of China

⁹ China University of Geosciences, Wuhan 430074, People's Republic of China

¹⁰ Chung-Ang University, Seoul, 06974, Republic of Korea

¹¹ COMSATS University Islamabad, Lahore Campus, Defence Road, Off Raiwind Road, 54000 Lahore, Pakistan

¹² Fudan University, Shanghai 200433, People's Republic of China

¹³ GSI Helmholtzcentre for Heavy Ion Research GmbH, D-64291 Darmstadt, Germany

¹⁴ Guangxi Normal University, Guilin 541004, People's Republic of China

¹⁵ Guangxi University, Nanning 530004, People's Republic of China

¹⁶ Hangzhou Normal University, Hangzhou 310036, People's Republic of China

¹⁷ Hebei University, Baoding 071002, People's Republic of China

¹⁸ Helmholtz Institute Mainz, Staudinger Weg 18, D-55099 Mainz, Germany

¹⁹ Henan Normal University, Xinxiang 453007, People's Republic of China

²⁰ Henan University, Kaifeng 475004, People's Republic of China

²¹ Henan University of Science and Technology, Luoyang 471003, People's Republic of China

²² Henan University of Technology, Zhengzhou 450001, People's Republic of China

²³ Huangshan College, Huangshan 245000, People's Republic of China

²⁴ Hunan Normal University, Changsha 410081, People's Republic of China

²⁵ Hunan University, Changsha 410082, People's Republic of China

²⁶ Indian Institute of Technology Madras, Chennai 600036, India

²⁷ Indiana University, Bloomington, Indiana 47405, USA

²⁸ INFN Laboratori Nazionali di Frascati , (A)INFN Laboratori Nazionali di Frascati, I-00044, Frascati, Italy; (B)INFN Sezione di Perugia, I-06100, Perugia, Italy; (C)University of Perugia, I-06100, Perugia, Italy

²⁹ INFN Sezione di Ferrara, (A)INFN Sezione di Ferrara, I-44122, Ferrara, Italy; (B)University of Ferrara, I-44122, Ferrara, Italy

³⁰ Inner Mongolia University, Hohhot 010021, People's Republic of China

³¹ Institute of Modern Physics, Lanzhou 730000, People's Republic of China

³² Institute of Physics and Technology, Peace Avenue 54B, Ulaanbaatar 13330, Mongolia

³³ Instituto de Alta Investigación, Universidad de Tarapacá, Casilla 7D, Arica 1000000, Chile

³⁴ Jilin University, Changchun 130012, People's Republic of China

³⁵ Johannes Gutenberg University of Mainz, Johann-Joachim-Becher-Weg 45, D-55099 Mainz, Germany

³⁶ Joint Institute for Nuclear Research, 141980 Dubna, Moscow region, Russia

³⁷ Justus-Liebig-Universitaet Giessen, II. Physikalisches Institut, Heinrich-Buff-Ring 16, D-35392 Giessen, Germany

³⁸ Lanzhou University, Lanzhou 730000, People's Republic of China

³⁹ Liaoning Normal University, Dalian 116029, People's Republic of China

⁴⁰ Liaoning University, Shenyang 110036, People's Republic of China

⁴¹ Nanjing Normal University, Nanjing 210023, People's Republic of China

- ⁴² Nanjing University, Nanjing 210093, People's Republic of China
⁴³ Nankai University, Tianjin 300071, People's Republic of China
⁴⁴ National Centre for Nuclear Research, Warsaw 02-093, Poland
⁴⁵ North China Electric Power University, Beijing 102206, People's Republic of China
⁴⁶ Peking University, Beijing 100871, People's Republic of China
⁴⁷ Qufu Normal University, Qufu 273165, People's Republic of China
⁴⁸ Renmin University of China, Beijing 100872, People's Republic of China
⁴⁹ Shandong Normal University, Jinan 250014, People's Republic of China
⁵⁰ Shandong University, Jinan 250100, People's Republic of China
⁵¹ Shanghai Jiao Tong University, Shanghai 200240, People's Republic of China
⁵² Shanxi Normal University, Linfen 041004, People's Republic of China
⁵³ Shanxi University, Taiyuan 030006, People's Republic of China
⁵⁴ Sichuan University, Chengdu 610064, People's Republic of China
⁵⁵ Soochow University, Suzhou 215006, People's Republic of China
⁵⁶ South China Normal University, Guangzhou 510006, People's Republic of China
⁵⁷ Southeast University, Nanjing 211100, People's Republic of China
⁵⁸ State Key Laboratory of Particle Detection and Electronics, Beijing 100049, Hefei 230026, People's Republic of China
⁵⁹ Sun Yat-Sen University, Guangzhou 510275, People's Republic of China
⁶⁰ Suranaree University of Technology, University Avenue 111, Nakhon Ratchasima 30000, Thailand
⁶¹ Tsinghua University, Beijing 100084, People's Republic of China
⁶² Turkish Accelerator Center Particle Factory Group, (A)Istinye University, 34010, Istanbul, Turkey; (B)Near East University, Nicosia, North Cyprus, 99138, Mersin 10, Turkey
⁶³ University of Bristol, (A)H H Wills Physics Laboratory; (B)Tyndall Avenue; (C)Bristol; (D)BS8 1TL
⁶⁴ University of Chinese Academy of Sciences, Beijing 100049, People's Republic of China
⁶⁵ University of Groningen, NL-9747 AA Groningen, The Netherlands
⁶⁶ University of Hawaii, Honolulu, Hawaii 96822, USA
⁶⁷ University of Jinan, Jinan 250022, People's Republic of China
⁶⁸ University of Manchester, Oxford Road, Manchester, M13 9PL, United Kingdom
⁶⁹ University of Muenster, Wilhelm-Klemm-Strasse 9, 48149 Muenster, Germany
⁷⁰ University of Oxford, Keble Road, Oxford OX13RH, United Kingdom
⁷¹ University of Science and Technology Liaoning, Anshan 114051, People's Republic of China
⁷² University of Science and Technology of China, Hefei 230026, People's Republic of China
⁷³ University of South China, Hengyang 421001, People's Republic of China
⁷⁴ University of the Punjab, Lahore-54590, Pakistan
⁷⁵ University of Turin and INFN, (A)University of Turin, I-10125, Turin, Italy; (B)University of Eastern Piedmont, I-15121, Alessandria, Italy; (C)INFN, I-10125, Turin, Italy
⁷⁶ Uppsala University, Box 516, SE-75120 Uppsala, Sweden
⁷⁷ Wuhan University, Wuhan 430072, People's Republic of China
⁷⁸ Yantai University, Yantai 264005, People's Republic of China
⁷⁹ Yunnan University, Kunming 650500, People's Republic of China
⁸⁰ Zhejiang University, Hangzhou 310027, People's Republic of China
⁸¹ Zhengzhou University, Zhengzhou 450001, People's Republic of China
- ^a Deceased
- ^b Also at the Moscow Institute of Physics and Technology, Moscow 141700, Russia
^c Also at the Novosibirsk State University, Novosibirsk, 630090, Russia
^d Also at the NRC "Kurchatov Institute", PNPI, 188300, Gatchina, Russia
^e Also at Goethe University Frankfurt, 60323 Frankfurt am Main, Germany
- ^f Also at Key Laboratory for Particle Physics, Astrophysics and Cosmology, Ministry of Education; Shanghai Key Laboratory for Particle Physics and Cosmology; Institute of Nuclear and Particle Physics, Shanghai 200240, People's Republic of China
- ^g Also at Key Laboratory of Nuclear Physics and Ion-beam Application (MOE) and Institute of Modern Physics, Fudan University, Shanghai 200443, People's Republic of China
- ^h Also at State Key Laboratory of Nuclear Physics and Technology, Peking University, Beijing 100871, People's Republic of China
- ⁱ Also at School of Physics and Electronics, Hunan University, Changsha 410082, China
- ^j Also at Guangdong Provincial Key Laboratory of Nuclear Science, Institute of Quantum Matter, South China Normal University, Guangzhou 510006, China
- ^k Also at MOE Frontiers Science Center for Rare Isotopes, Lanzhou University, Lanzhou 730000, People's Republic of China
- ^l Also at Lanzhou Center for Theoretical Physics, Lanzhou University, Lanzhou 730000, People's Republic of China
- ^m Also at the Department of Mathematical Sciences, IBA, Karachi 75270, Pakistan
- ⁿ Also at Ecole Polytechnique Federale de Lausanne (EPFL), CH-1015 Lausanne, Switzerland
- ^o Also at Helmholtz Institute Mainz, Staudinger Weg 18, D-55099 Mainz, Germany

Using 7.93 fb^{-1} of e^+e^- collision data collected at a center-of-mass energy of 3.773 GeV with the BESIII detector, we present an analysis of the decay $D^0 \rightarrow \eta\pi^-e^+\nu_e$. The branching fraction of the decay $D^0 \rightarrow a_0(980)^-e^+\nu_e$ with $a_0(980)^-\rightarrow\eta\pi^-$ is measured to be $(0.86\pm0.17_{\text{stat}}\pm0.05_{\text{syst}})\times10^{-4}$. The decay dynamics of this process is studied with a single-pole parameterization of the hadronic form factor and the Flatté formula describing the $a_0(980)$ line shape in the differential decay rate. The product of the form factor $f_+^{a_0}(0)$ and the Cabibbo-Kobayashi-Maskawa matrix element $|V_{cd}|$ is determined for the first time with the result $f_+^{a_0}(0)|V_{cd}| = 0.126 \pm 0.013_{\text{stat}} \pm 0.003_{\text{syst}}$.

Understanding the nature of scalar mesons has emerged as a pivotal challenge within the realm of non-perturbative quantum chromodynamics (QCD), given their important role in dynamically generating mass via the spontaneous breaking of QCD's chiral symmetry. Consequently, a thorough understanding of the phenomenon of confinement physics necessitates a deep exploration of the nature of these mesons [1, 2]. The existence of light scalar mesons (S_0) below 1 GeV , including the $K_0^*(700)$, $f_0(500)$ (σ), $f_0(980)$ (f_0), and $a_0(980)$ (a_0), has been firmly established.

The constituent quark model has been strikingly successful in the identification of the nonets of pseudo-scalar, vector and tensor mesons over the past decades [3]. However, the classification of scalar mesons with $J^{PC} = 0^{++}$ remains a long-standing puzzle, particularly due to the challenges encountered in describing them as normal quark-antiquark ($q\bar{q}$) states. The two-quark model expects that the non-strange-flavored $a_0(980)$ should be as light as the σ meson, whereas experimentally it is mixed with the strange-flavored $f_0(980)$. Several experimental observations have notably intensified the discrepancies with the conventional $q\bar{q}$ interpretation. The decay $\phi \rightarrow \gamma a_0(980)^0$, which violates both charge conjugation and parity conservation, is also observed with an anomalously large branching fraction (BF) [3, 4]. In addition, the BESIII collaboration measured the BFs of the $D_s^+ \rightarrow a_0(980)^{0(+)}\pi^{+(0)}$ [5], $D_s^+ \rightarrow a_0(980)^{0(+)}\rho^{+(0)}$ [6] and $D^{0(+)} \rightarrow a_0(980)^{+}\pi^{-0)}$ [7] decays to be much larger than the expectations based on the naive two-quark model [8–10].

Various structure hypotheses have been proposed to explain these intriguing phenomena of scalar particles, including compact tetraquark states ($q^2\bar{q}^2$) [2, 11–14], two-meson molecule bound states [15–17], and mixed states [4]. Nevertheless, the intricate interplay of non-perturbative strong interactions, combined with the scalar mesons sharing the same spin-parity quantum numbers as the QCD vacuum, leads to significant hadronic uncertainties in their classification.

Semileptonic (SL) D decays offers a laboratory where the mechanism of the $D \rightarrow S_0$ transition can be cleanly studied, as the colorless lepton pair is not sensitive to the strong interaction [18–20]. In particular, the form factor (FF) of the $D \rightarrow S_0$ transition can be measured to provide a novel insight into the non-perturbative QCD effects on hadronization. Moreover, under the con-

straints of SU(3) flavor symmetry, the variation in the value of the $f_0\sigma$ mixing angle that are expected under different models leads to differences in the decay properties of $D \rightarrow S_0 e^+\nu_e$. In particular, the BF of the $D \rightarrow a_0(980)e^+\nu_e$ decay is a useful observable to distinguish between different descriptions of light scalar mesons [19, 20]. Consequently, the $D \rightarrow a_0(980)e^+\nu_e$ decay not only offers an ideal probe into the nature of $a_0(980)$, but also gives the opportunity for gaining a deeper understanding of the nature of the $f_0(500)$ and $f_0(980)$.

BESIII collaboration reported the observation of $D^0 \rightarrow a_0(980)^-e^+\nu_e$ with a 25% uncertainty in the measurement of its BF [21, 22] using 2.93 fb^{-1} data at $\sqrt{s} = 3.773 \text{ GeV}$. This discovery stimulated many theoretical studies and interpretations [19, 23–27]. The $\psi(3770)$ decays predominantly to $D^0\bar{D}^0$ or $D^+\bar{D}^-$ pairs without any additional hadrons. The excellent tracking, precision calorimetry, and the large $D\bar{D}$ threshold data sample [28] provide an unprecedented opportunity to accurately study the decay dynamics of $D^0 \rightarrow a_0(980)^-e^+\nu_e$. Based on a data set corresponding to an integrated luminosity of 7.93 fb^{-1} [29, 30], this Letter reports an improved measurement of the BF for the $D^0 \rightarrow a_0(980)^-e^+\nu_e$ decay, along with the first-ever measurement of the FF for the $D \rightarrow a_0(980)$ transition. Charge-conjugate modes are implied throughout this Letter.

The BESIII detector [28] records the final-state particles of symmetric e^+e^- collisions provided from the BEPCII storage ring [31] in the center-of-mass (CM) energy range from 1.85 to 4.95 GeV , with a peak luminosity of $1.1 \times 10^{33} \text{ cm}^{-2}\text{s}^{-1}$ achieved at $\sqrt{s} = 3.773 \text{ GeV}$. The cylindrical core of the BESIII detector covers 93% of the full solid angle and consists of a helium-based multilayer drift chamber (MDC), a plastic scintillator time-of-flight system (TOF), and a CsI(Tl) electromagnetic calorimeter (EMC), which are all enclosed in a superconducting solenoidal magnet providing a 1.0 T magnetic field.

Simulated data samples produced with a GEANT4-based [32] Monte Carlo (MC) toolkit, which includes the geometric description [33] of the BESIII detector and the detector response, are used to determine detection efficiencies and to estimate backgrounds. The simulation includes the beam-energy spread and initial-state radiation (ISR) in e^+e^- annihilations, which are generated with KKMC [34]. The inclusive sample includes the

production of $D\bar{D}$ pairs (including quantum coherence for the neutral D channels), the non- $D\bar{D}$ decays of the $\psi(3770)$, the ISR production of the J/ψ and $\psi(3686)$ states, and continuum processes. All particle decays are modeled with EVTGEN [35, 36] using BFs either taken from the Particle Data Group (PDG) [3], when available, or otherwise estimated with LUNDCHARM [37, 38]. Final-state radiation from charged final-state particles is incorporated using PHOTOS [39]. Since no significant non-resonance contribution is observed, we assume that the S-wave component of the $\eta\pi$ system solely receives contribution from the $a_0(980)$. The $D^0 \rightarrow \eta\pi^-e^+\nu_e$ decay can be simulated according to prior measurements on SL D decays [40, 41]. The $a_0(980)$ line shape is modeled by the Flatté formula with its parameters fixed to the BESIII measurement [42].

The double-tag (DT) method [43] provides high-purity samples for measuring the absolute BFs of D meson decays, without the need of knowing the integrated luminosity and the $D\bar{D}$ production cross section. The \bar{D}^0 mesons are first reconstructed in one of the three decay modes $K^+\pi^-$, $K^+\pi^-\pi^0$, and $K^+\pi^-\pi^+\pi^-$, referred to as single-tag (ST) events. After a \bar{D}^0 meson is found, the $D^0 \rightarrow \eta\pi^-e^+\nu_e$ candidate is searched for on the recoil side, where the presence of the undetected ν_e is inferred from the missing momentum. An event in which a signal $D^0 \rightarrow \eta\pi^-e^+\nu_e$ decay and an ST \bar{D}^0 is simultaneously found is referred to as a DT event.

The BF of the signal decay is determined by

$$\mathcal{B} = \frac{N_{\text{DT}}}{\sum_{\alpha} (N_{\text{ST}}^{\alpha} \epsilon_{\text{DT}}^{\alpha} / \epsilon_{\text{ST}}^{\alpha}) \mathcal{B}_{\text{sub}}}, \quad (1)$$

where α denotes the tag mode, N_{ST}^{α} is the ST yield for tag mode α , N_{DT} is the sum of the DT yields from all ST modes, while $\epsilon_{\text{ST}}^{\alpha}$ and $\epsilon_{\text{DT}}^{\alpha}$ refer to the corresponding efficiencies as determined from MC simulation. \mathcal{B}_{sub} represent the BFs of all possible daughter particles.

In isolating the ST samples, the selection criteria of K^{\pm} , π^{\pm} , and π^0 candidates are the same as Ref. [44]. The tagged \bar{D}^0 mesons are selected using the energy difference $\Delta E \equiv E_{\bar{D}^0} - E_{\text{beam}}$ and the beam-constrained mass $M_{\text{BC}} \equiv \sqrt{E_{\text{beam}}^2/c^4 - |\vec{p}_{\bar{D}^0}|^2/c^2}$, where E_{beam} is the beam energy, and $\vec{p}_{\bar{D}^0}$ and $E_{\bar{D}^0}$ are the measured momentum and energy of the \bar{D}^0 candidate in the e^+e^- rest frame, respectively. In the case of multiple candidates in an event, the one with the minimum $|\Delta E|$ is chosen. The ST yields and efficiencies are determined by fitting the M_{BC} distributions of the accepted candidates in data and inclusive MC sample, respectively. More details about the ST selection can be found in Ref. [44]. The ST yields in the data and the corresponding ST efficiencies are listed in Table I. Summing over all three tag modes, the total ST yield $N_{\text{ST}}^{\text{tot}}$ is $(6306.7 \pm 2.9) \times 10^3$ within the M_{BC} signal region, ranging from 1.859 to 1.873 GeV/c^2 .

TABLE I. The energy difference (ΔE) windows, ST yields in data (N_{ST}^{α}), ST efficiencies ($\epsilon_{\text{ST}}^{\alpha}$), DT efficiencies ($\epsilon_{\text{DT}}^{\alpha}$), with statistical uncertainties, for each tag mode α . These efficiencies do not include the BFs of all possible daughter particles.

Tag mode	ΔE (MeV)	$N_{\text{ST}}^{\alpha} (\times 10^3)$	$\epsilon_{\text{ST}}^{\alpha}(\%)$	$\epsilon_{\text{DT}}^{\alpha}(\%)$
$K^+\pi^-$	[-27, 27]	1449.3 ± 1.3	65.34 ± 0.01	17.20 ± 0.02
$K^+\pi^-\pi^0$	[-62, 49]	2913.2 ± 2.0	35.59 ± 0.01	8.88 ± 0.01
$K^+\pi^-\pi^+\pi^-$	[-26, 24]	1944.2 ± 1.6	40.83 ± 0.01	8.81 ± 0.01

Once a ST \bar{D}^0 decay has been identified, a search is made for a D^0 signal decay in the same event. Candidate η , π^- and e^+ are selected with the remaining charged tracks and photon candidates. The selection criteria for π^{\pm} , e^{\pm} and photon candidates are the same as in Ref. [44]. The η candidates are reconstructed through the decay $\eta \rightarrow \gamma\gamma$, requiring the invariant mass ($M_{\gamma\gamma}$) to lie within the range $(0.505, 0.575)$ GeV/c^2 . A one-constraint kinematic fit is performed, constraining $M_{\gamma\gamma}$ to the known η mass [3], and the combination giving the minimum χ^2_{IC} is kept for further analysis. Furthermore, DT candidates are rejected if they contain any extra charged tracks ($N_{\text{extra}}^{\text{char}}$) or π^0 reconstructed with unused photons ($N_{\text{extra}}^{\pi^0}$). This π^0 veto effectively suppresses the backgrounds arising from $D^0 \rightarrow \pi^-\pi^0e^+\nu_e$ and $D^0 \rightarrow K^*(892)^-e^+\nu_e$ with the subsequent decay $K^*(892)^- \rightarrow K_S^0(\rightarrow \pi^0\pi^0)\pi^-$. An additional background comes from $D^0 \rightarrow K^*(892)^-e^+\nu_e$ decays, followed by $K^*(892)^- \rightarrow K_L^0\pi^-$, where the EMC shower induced by the K_L^0 mimics the higher-energy photon of the η candidate. To suppress these events, the lateral moment [45] of EMC showers, which peaks around 0.15 for real photons but varies from 0 to 0.85 for K_L^0 candidates, is required to lie within $(0, 0.35)$ for the higher-energy photon from the η candidate. This requirement suppresses about 78% of the K_L^0 background while retaining 93% of the signal.

The energy and momentum of the undetectable neutrino in the e^+e^- CM frame are derived as $E_{\text{miss}} \equiv E_{\text{beam}} - \sum_i E_i$ and $\vec{p}_{\text{miss}} \equiv -(\vec{p}_{\text{tag}} + \sum_i \vec{p}_i)$, respectively, where E_i and \vec{p}_i are the energy and momentum of the η , π^- , e^+ of the signal side. We calculate $\vec{p}_{\text{tag}} = \hat{p}_{\text{tag}} \sqrt{E_{\text{beam}}^2 - m_{D^0}^2 c^4}$, where \hat{p}_{tag} is the unit vector in the momentum direction of the ST D^0 and m_{D^0} is the known D^0 mass [3]. The signal candidates are expected to peak around zero in the $U_{\text{miss}} \equiv E_{\text{miss}} - c|\vec{p}_{\text{miss}}|$ distribution and near the nominal mass of $a_0(980)$ in the $\eta\pi^-$ mass spectrum ($M_{\eta\pi^-}$). To obtain the signal yields, we perform two-dimensional (2D) unbinned maximum likelihood fits to the U_{miss} versus $M_{\eta\pi^-}$ distributions. The signal shape in the U_{miss} distribution is described by the MC simulation and that in the $M_{\eta\pi^-}$ distribution is modeled with a standard Flatté formula [46] for the $a_0(980)$ signal, using 0.990 GeV/c^2 for the $a_0(980)$ mass (m_0). Here we

assume that $a_0(980)$ decays only to $\eta\pi$ and $K\bar{K}$ final states, with the corresponding coupling constants fixed at $g_{\eta\pi}^2 = 0.341 \text{ (GeV}/c^2)^2$ and $g_{K\bar{K}}^2 = 0.304 \text{ (GeV}/c^2)^2$, respectively [42]. The background is described by the shape found in the inclusive MC sample. The 2D probability density functions of all these components are constructed by the product of the U_{miss} and $M_{\eta\pi}$ functions. Studies performed with the inclusive MC simulation shows that there is a negligible correlation between these two observables. Projections of the 2D fits are shown in Fig. 1. Without considering the non-resonant contribution, the measured signal yield is $N_{\text{DT}} = 51.8 \pm 10.0$ with a statistical significance of 6.9σ . The statistical significance is given by $\sqrt{-2\ln(\mathcal{L}_0/\mathcal{L})}$, where \mathcal{L} and \mathcal{L}_0 are the maximum likelihood values with the signal yield has a free parameter and fixed to zero, respectively. The corresponding DT efficiencies are presented in Table I.

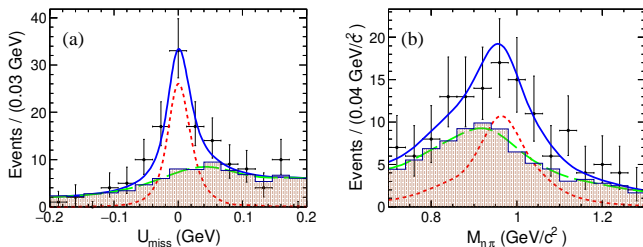


FIG. 1. Projections of the 2D fit on U_{miss} (a) and $M_{\eta\pi^-}$ (b) for $D^0 \rightarrow a_0(980)^- e^+ \nu_e$. The points with error bars are data. The (blue) solid curves are the overall fits, the (red) short-dashed lines show the fitted signal shape; the (green) long-dashed lines denote the background shape. The (dark red) histogram is the MC simulated background.

The systematic uncertainties in the BF measurement are summarized in Table I of Ref. [47], and discussed below. The uncertainty in the ST \bar{D}^0 yield reflects the uncertainty in the fit to the M_{BC} distributions and is assessed by varying the signal and background shapes. The uncertainties in the tracking or PID efficiencies of π^- and e^+ are studied with control samples of DT-hadronic events and $e^+e^- \rightarrow \gamma e^+e^-$, respectively. Due to the consistency in the overall reconstruction efficiency between η and π^0 , the uncertainty associated with the η reconstruction and $N_{\text{extra}}^{\pi^0}$ requirement are both assigned by studying a control sample of $D^0 \rightarrow K^-\pi^+\pi^0$ decays. The efficiency of the lateral moment requirement for photons is studied in different energy and polar-angle bins using a control sample of $e^+e^- \rightarrow \gamma e^+e^-$ events. The efficiency correction factors for these sources are determined by measuring the differences in efficiency between the MC and data control samples, which are weighted based on the distributions of several common kinematic variables, including energy, momentum, and polar angle, of the signal MC sample. The resulting systematic uncertainties are then propagated from the statistical un-

certainties of the control samples. The uncertainty arising from the signal model is estimated by measuring the BF difference when changing the line shape parameters of the $a_0(980)$ measured by BESIII collaboration [42] to the one measured by CLEO-c collaboration [48] in the signal MC generator. The uncertainty of the background shape is assessed by altering the baseline MC background shape with two methods, and subsequently combining the uncertainties derived from these alterations to represent the overall uncertainty. Firstly, to account for the imperfect agreement between data and MC simulation for K_L^0 reconstruction, we increase the yield of the major background process $D^0 \rightarrow K^*(892)^- e^+ \nu_e$ with $K^*(892)^- \rightarrow K_L^0 \pi^-$ by 30%, based on the analysis of control samples $D^0 \rightarrow K_L^0 \pi^+ \pi^-$, $D^0 \rightarrow K_L^0 \pi^+ \pi^- \pi^0$ and $D^+ \rightarrow K_L^0 \pi^+ \pi^0$ decays. Secondly, the $e^+e^- \rightarrow q\bar{q}$ background yields are changed by $\pm 1\sigma$ of the measured cross section [49]. In order to assign a systematic uncertainty associated with the modelling of the resolution of U_{miss} , the fit is reperformed with the signal shape convolved with a Gaussian function. The width of the Gaussian distribution, which represents the resolution difference between experimental data and MC simulation, is fixed based on the estimation derived from the control sample of the decay process $D^0 \rightarrow \pi^0 \pi^- e^+ \nu_e$. Changes in the signal yields are assigned to be the corresponding uncertainties. The uncertainty associated with the assumed BF of the η decay is taken from Ref. [3]. The effect of the limited MC sample size is also included as a systematic effect. Assuming that all sources are independent, the total systematic uncertainty on the BF is determined to be 5.2%, by adding them in quadrature.

To extract the hadronic FF of the $D \rightarrow a_0(980)$ transition, the signal candidate events are divided into three intervals of q^2 (the four-momentum transfer squared of the $e^+ \nu_e$ system) and a χ^2 fit is used to determine the partial decay rates. Considering the correlations of the measured partial decay rates ($\Delta\Gamma_{\text{mea}}^i$) among different q^2 intervals, the χ^2 is given by

$$\chi^2 = \sum_{ij} (\Delta\Gamma_{\text{mea}}^i - \Delta\Gamma_{\text{exp}}^i) [C^{-1}]_{ij} (\Delta\Gamma_{\text{mea}}^j - \Delta\Gamma_{\text{exp}}^j), \quad (2)$$

where $\Delta\Gamma_{\text{mea}}^i$ and $\Delta\Gamma_{\text{exp}}^i$ represent the measured and theoretically expected partial decay rates, respectively, in the i -th q^2 interval. Here, the indices i and j denote different q^2 intervals. The elements of the inverse covariance matrix C^{-1} , denoted as $[C^{-1}]_{ij}$, account for the correlations between the different q^2 bins.

The $\Delta\Gamma_{\text{exp}}^i$ are calculated by integrating the following double differential decay rate [50, 51]:

$$\begin{aligned} & \frac{d^2\Gamma(D^0 \rightarrow a_0(980)^- e^+ \nu_e)}{ds dq^2} \\ &= \frac{G_F^2 |V_{cd}|^2}{192\pi^4 m_{D^0}^3} \lambda^{3/2} (m_{D^0}^2, s, q^2) |f_+^{a_0}(q^2)|^2 P(s), \end{aligned} \quad (3)$$

where s is the square of $M_{\eta\pi}$, G_F is the Fermi constant [3], V_{cd} is the Cabibbo-Kobayashi-Maskawa matrix element, m_{D^0} is the known D^0 mass [3], $\lambda(x, y, z) = x^2 + y^2 + z^2 - 2xy - 2xz - 2yz$, and $P(s)$ is based on the relativistic Flatté formula [46, 48]:

$$P(s) = \frac{g_{\eta\pi}^2 \rho_{\eta\pi}}{|m_0^2 - s - i(g_{\eta\pi}^2 \rho_{\eta\pi} + g_{K\bar{K}}^2 \rho_{K\bar{K}})|^2}, \quad (4)$$

where $\rho_{\eta\pi}$ and $\rho_{K\bar{K}}$ are individual phase-space factors. The product of the FF and $|V_{cd}|$ is extracted in three intervals of q^2 . The FF is modeled with the single-pole parameterization [52]:

$$f_+^{a_0}(q^2) = \frac{f_+^{a_0}(0)}{1 - \frac{q^2}{m_{\text{pole}}^2}}, \quad (5)$$

where $f_+^{a_0}(0)$ is the FF evaluated at $q^2 = 0 \text{ GeV}^2/c^4$, and the pole mass $m_{\text{pole}} = 2.42 \text{ GeV}/c^2$ [3, 53].

The measured partial decay rate $\Delta\Gamma_{\text{mea}}^i$ is determined by $\Delta\Gamma_{\text{mea}}^i = N_{\text{pro}}^i / (\tau N_{\text{ST}}^{\text{tot}})$, where τ is the D^0 -meson lifetime [3] and N_{pro}^i is the signal yield produced in the i -th q^2 interval, given by $N_{\text{pro}}^i = \sum_{j=1}^3 [\epsilon^{-1}]_{ij} N_{\text{obs}}^j$. The N_{obs}^j is the observed signal yield obtained from the 2D fits on the U_{miss} versus $M_{\eta\pi^-}$ distribution in the j -th q^2 interval, carried out in a similar manner as the one described previously for the BF measurement. The matrix ϵ^{-1} represents the inverse of the efficiency matrix. ϵ_{ij} is the efficiency matrix element determined from the signal MC samples via $\epsilon_{ij} = \sum_k [(1/N_{\text{ST}}^{\text{tot}}) \times (N_{\text{rec}}^{ij}/N_{\text{gen}}^j)_k \times (N_{\text{ST}}^k/\epsilon_{\text{ST}}^k)]$, where N_{rec}^{ij} is the number of signal events reconstructed in the i -th q^2 interval while generated in the j -th q^2 interval, N_{gen}^j represents the generated number of signal events in the j -th q^2 interval, and k sums over all tag modes. The details of the q^2 divisions, N_{obs}^i , N_{pro}^i , and $\Delta\Gamma_{\text{mea}}^i$ are given in Table II.

TABLE II. The partial decay rates of $D^0 \rightarrow a_0(980)^- e^+ \nu_e$, $a_0(980)^- \rightarrow \eta\pi^-$ in different q^2 intervals, where the uncertainties are statistical only.

i	$q^2(\text{GeV}^2/c^4)$	N_{obs}^i	N_{pro}^i	$\Delta\Gamma_{\text{mea}}^i(\text{ns}^{-1})$
1	[0.0, 0.2]	16.9 ± 5.7	75.6 ± 27.0	0.074 ± 0.027
2	[0.2, 0.4]	15.5 ± 5.0	63.1 ± 22.4	0.062 ± 0.022
3	[0.4, q_{max}^2]	17.4 ± 5.9	67.6 ± 23.8	0.066 ± 0.023

The statistical and systematic covariance matrices are constructed as $C_{ij}^{\text{stat}} = (\frac{1}{\tau N_{\text{ST}}^{\text{tot}}})^2 \sum_{\alpha} \epsilon_{i\alpha}^{-1} \epsilon_{j\alpha}^{-1} \sigma^2(N_{\text{obs}}^{\alpha})$ and $C_{ij}^{\text{syst}} = \delta(\Delta\Gamma_{\text{mea}}^i) \delta(\Delta\Gamma_{\text{mea}}^j)$, respectively, where $\sigma(N_{\text{obs}}^{\alpha})$ and $\delta(\Delta\Gamma_{\text{mea}}^i)$ are the statistical and systematic uncertainties in the i -th q^2 interval. The C_{ij}^{syst} elements are obtained by summing all the covariance matrices for all systematic uncertainties, where the systematic uncertainty of τ , 0.2% [3], is included in addition to those in the BF measurement and are given in Ref. [47].

The systematic uncertainty related to $\Delta\Gamma_{\text{mea}}^i$ is estimated to be 2.4% by following Ref. [54]. In addition, the input parameters m_0 , $g_{\eta\pi}^2$ and $g_{K\bar{K}}^2$ related to $\Delta\Gamma_{\text{exp}}^i$ are also considered by varying them within $\pm 1\sigma$ from their central values [42]. The largest deviations of the form factor, respectively 0.2%, 0.1% and 0.6%, are taken as systematic uncertainties. The quadrature sum of these uncertainties is 2.7%, and is taken as the total systematic uncertainty.

A fit is performed for the differential decay rate measured through the process $D^0 \rightarrow a_0(980)^- e^+ \nu_e$ and the results are presented in Figs. 2 (a) and (b) where the fitted decay rate and its projection onto the hadronic FF. The goodness-of-fit is $\chi^2/\text{NDOF} = 2.2/2 = 1.1$, where NDOF is the number of degrees of freedom. The product $f_+^{a_0}(0)|V_{cd}|$ is determined to be $0.126 \pm 0.013_{\text{stat}} \pm 0.003_{\text{syst}}$. The baseline FF is taken from the fit with the combined statistical and systematic covariance matrix, and the statistical uncertainty on the FF is taken from the fit with only the statistical covariance matrix. The systematic uncertainty is obtained by calculating the quadratic difference of uncertainties between these two fits.

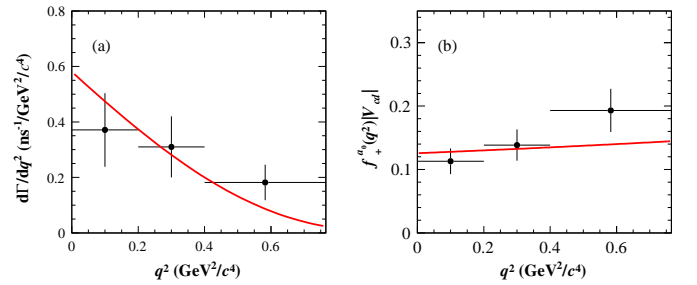


FIG. 2. Fit to the differential decay rate as function of q^2 (a) and projection to the FF $f_+^{a_0}(q^2)|V_{cd}|$ (b). The points with error bars are data, and the red solid line is the fit.

Using e^+e^- collision data corresponding to an integrated luminosity of 7.91 fb^{-1} collected with the BE-SIII detector at $\sqrt{s} = 3.773 \text{ GeV}$, this Letter reports the absolute BF of the decay $D^0 \rightarrow a_0(980)^- e^+ \nu_e$ with $a_0(980)^- \rightarrow \eta\pi^-$ to be $(0.86 \pm 0.17_{\text{stat}} \pm 0.05_{\text{syst}}) \times 10^{-4}$, which is 1.2 times more precise than the previous measurement [21] and exhibits some tension with theoretical predictions, as shown in Table III.

We have also investigated the dynamics of the decay $D^0 \rightarrow a_0(980)^- e^+ \nu_e$ and measured the product $f_+^{a_0}(0)|V_{cd}| = 0.126 \pm 0.013_{\text{stat}} \pm 0.003_{\text{syst}}$ for the first time by parametrizing the FF using a single-pole model. With the value of $|V_{cd}| = 0.22486 \pm 0.00067$ from the standard model global fit [3] as input, we determine $f_+^{a_0}(0) = 0.559 \pm 0.056_{\text{stat}} \pm 0.013_{\text{syst}}$. Table III shows that these results are consistent with the CCQM [23], SU(3) flavor symmetry [19] calculations within 2σ , but

disfavor the Ads/QCD [24] and LCSR calculations [25–27] by more than 2σ .

The measured BF of $D^0 \rightarrow a_0(980)^- e^+ \nu_e$ and the FF of D to $a_0(980)$ transition will serve as an important input for understanding the intricate internal structure of the light scalar mesons [19, 20]. The measurement of $f_+^{a_0}(0)$ has additional importance in the information it gives on the direct hadronization of the D to $a_0(980)$ transition. This information is essential input for performing an accurate calculation of the ratio of external W -emission and W -annihilation contributions in the quasi-two-body $D \rightarrow SP$ sector when estimating the contributions from final-state interactions [55]. In the near future, an investigation based on the full 20 fb^{-1} of data now available at BESIII detector will enable a more precise exploration of the production of light scalar states in the SL decays of D mesons [22, 56, 57].

The BESIII Collaboration thanks the staff of BEPCII and the IHEP computing center for their strong support. This work is supported in part by National Key R&D Program of China under Contracts Nos. 2023YFA1606000, 2020YFA0406400, 2020YFA0406300; National Natural Science Foundation of China (NSFC) under Contracts Nos. 11635010, 11735014, 11935015, 11935016, 11935018, 12025502, 12035009, 12035013, 12061131003, 12192260, 12192261, 12192262, 12192263, 12192264, 12192265, 12221005, 12225509, 12235017, 12361141819; the Chinese Academy of Sciences (CAS) Large-Scale Scientific Facility Program; the CAS Center for Excellence in Particle Physics (CCEPP); Joint Large-Scale Scientific Facility Funds of the NSFC and CAS under Contract No. U2032104, U1832207; 100 Talents Program of CAS; the Excellent Youth Foundation of Henan Scientific Committee under Contract No. 242300421044; The Institute of Nuclear and Particle Physics (INPAC) and Shanghai Key Laboratory for Particle Physics and Cosmology; German Research Foundation DFG under Contracts Nos. FOR5327, GRK 2149; Istituto Nazionale di Fisica Nucleare, Italy; Knut and Alice Wallenberg Foundation under Contracts Nos. 2021.0174, 2021.0299; Ministry of Development of Turkey under Contract No. DPT2006K-120470; National Research Foundation of Korea under Contract No. NRF-2022R1A2C1092335; National Science and Technology fund of Mongolia; National Science Research and Innovation Fund (NSRF) via the Program Management Unit for Human Resources & Institutional Development, Research and Innovation of Thailand under Contracts Nos. B16F640076, B50G670107; Polish National Science Centre under Contract No. 2019/35/O/ST2/02907; Swedish Research Council under Contract No. 2019.04595; The Swedish Foundation for International Cooperation in Research and Higher Education under Contract No. CH2018-7756; U. S. Department of Energy under Contract No. DE-FG02-05ER41374.

-
- [1] N. N. Achasov and A. V. Kislev, Phys. Rev. D **98**, 096009 (2018), arXiv:1805.10145 [hep-ph].
 - [2] R. L. Jaffe, Phys. Rev. D **15**, 267 (1977).
 - [3] S. Navas *et al.* (Particle Data Group), Phys. Rev. D **110**, 030001 (2024).
 - [4] F. L. Braghin, J. Phys. G **50**, 095101 (2023), arXiv:2212.06616 [hep-ph].
 - [5] M. Ablikim *et al.* (BESIII Collaboration), Phys. Rev. Lett. **123**, 112001 (2019), arXiv:1903.04118 [hep-ex].
 - [6] M. Ablikim *et al.* (BESIII Collaboration), Phys. Rev. D **104**, L071101 (2021), arXiv:2106.13536 [hep-ex].
 - [7] M. Ablikim *et al.* (BESIII Collaboration), (2024), arXiv:2404.09219 [hep-ex].
 - [8] Y.-K. Hsiao, Y. Yu, and B.-C. Ke, Eur. Phys. J. C **80**, 895 (2020), arXiv:1909.07327 [hep-ph].
 - [9] Y. Yu, Y.-K. Hsiao, and B.-C. Ke, Eur. Phys. J. C **81**, 1093 (2021), arXiv:2108.02936 [hep-ph].
 - [10] M.-Y. Duan, J.-Y. Wang, G.-Y. Wang, E. Wang, and D.-M. Li, Eur. Phys. J. C **80**, 1041 (2020), arXiv:2008.10139 [hep-ph].
 - [11] T. V. Brito, F. S. Navarra, M. Nielsen, and M. E. Bracco, Phys. Lett. B **608**, 69 (2005), arXiv:hep-ph/0411233.
 - [12] E. Klemt and A. Zaitsev, Phys. Rept. **454**, 1 (2007), arXiv:0708.4016 [hep-ph].
 - [13] C. Alexandrou, J. Berlin, M. Dalla Brida, J. Finkenrath, T. Leontiou, and M. Wagner, Phys. Rev. D **97**, 034506 (2018), arXiv:1711.09815 [hep-lat].
 - [14] T. Humanic *et al.* (ALICE Collaboration), Rev. Mex. Fis. Suppl. **3**, 0308039 (2022).
 - [15] J. D. Weinstein and N. Isgur, Phys. Rev. Lett. **48**, 659 (1982).
 - [16] L.-Y. Dai and M. R. Pennington, Phys. Lett. B **736**, 11 (2014), arXiv:1403.7514 [hep-ph].
 - [17] T. Sekihara and S. Kumano, Phys. Rev. D **92**, 034010 (2015), arXiv:1409.2213 [hep-ph].
 - [18] M. A. Ivanov, J. G. Körner, J. N. Pandya, P. Santorelli, N. R. Soni, and C.-T. Tran, Front. Phys. **14**, 64401 (2019), arXiv:1904.07740 [hep-ph].
 - [19] Y.-K. Hsiao, S.-Q. Yang, W.-J. Wei, and B.-C. Ke, (2023), arXiv:2306.06091 [hep-ph].
 - [20] W. Wang and C.-D. Lu, Phys. Rev. D **82**, 034016 (2010), arXiv:0910.0613 [hep-ph].
 - [21] M. Ablikim *et al.* (BESIII Collaboration), Phys. Rev. Lett. **121**, 081802 (2018), arXiv:1803.02166 [hep-ex].
 - [22] B.-C. Ke, J. Koponen, H.-B. Li, and Y. Zheng, Ann. Rev. Nucl. Part. Sci. **73**, 285 (2023), arXiv:2310.05228 [hep-ex].
 - [23] N. R. Soni, A. N. Gadaria, J. J. Patel, and J. N. Pandya, Phys. Rev. D **102**, 016013 (2020), arXiv:2001.10195 [hep-ph].
 - [24] S. Momeni and M. Saghebifar,

TABLE III. Comparisons of $f_+^{a_0}(0)$ and $\mathcal{B}(D^0 \rightarrow a_0(980)^- e^+ \nu_e, a_0(980)^- \rightarrow \eta \pi^-)$ between our measurements, previous measurements, and various theoretical predictions. Assuming that the $a_0(980)$ width is saturated by the $K\bar{K}$ and $\eta\pi$ modes, $\mathcal{B}(a_0(980) \rightarrow \eta\pi)$ can be inferred from the PDG average value of $\Gamma(a_0(980) \rightarrow K\bar{K})/\Gamma(a_0(980) \rightarrow \eta\pi) = 0.172 \pm 0.019$ [3]. The narrow width approximation is further applied to estimate the \mathcal{B} for uncomputed cases (denoted by the superscript *).

	$f_+^{a_0}(0)$	$\mathcal{B}(D^0 \rightarrow a_0(980)^- e^+ \nu_e, a_0(980)^- \rightarrow \eta \pi^-) (\times 10^{-4})$
CCQM [23]	$0.55^{+0.02}_{-0.02}$	$1.43 \pm 0.13^*$
Ads/QCD [24]	0.72 ± 0.09	$2.08 \pm 0.26^*$
LCSR 2017 [25]	$1.75^{+0.26}_{-0.27}$	$3.48^{+1.17}_{-1.04}^*$
LCSR 2021 [26]	$0.85^{+0.10}_{-0.11}$	1.15
LCSR 2023 [27]	$1.070^{+0.066}_{-0.033}$	$1.330^{+0.216}_{-0.134}$
SU(3) flavor symmetry [19]	0.46 ± 0.06	...
BESIII 2018 [21]	...	$1.33^{+0.33}_{-0.29\text{stat}} \pm 0.09\text{syst}$
This work	$0.559 \pm 0.056\text{stat} \pm 0.013\text{syst}$	$0.86 \pm 0.17\text{stat} \pm 0.05\text{syst}$

- Eur. Phys. J. C **82**, 473 (2022).
- [25] X.-D. Cheng, H.-B. Li, B. Wei, Y.-G. Xu, and M.-Z. Yang, Phys. Rev. D **96**, 033002 (2017), arXiv:1706.01019 [hep-ph].
- [26] Q. Huang, Y.-J. Sun, D. Gao, G.-H. Zhao, B. Wang, and W. Hong, (2021), arXiv:2102.12241 [hep-ph].
- [27] Z.-H. Wu, H.-B. Fu, T. Zhong, D. Huang, D.-D. Hu, and X.-G. Wu, Nucl. Phys. A **1036**, 122671 (2023), arXiv:2211.05390 [hep-ph].
- [28] M. Ablikim *et al.* (BESIII Collaboration), Nucl. Instrum. Meth. A **614**, 345 (2010), arXiv:0911.4960 [physics.ins-det].
- [29] M. Ablikim *et al.* (BESIII Collaboration), Chin. Phys. C **37**, 123001 (2013), arXiv:1307.2022 [hep-ex].
- [30] M. Ablikim *et al.* (BESIII), (2024), arXiv:2406.05827 [hep-ex].
- [31] C. Yu *et al.*, in *7th International Particle Accelerator Conference* (2016) p. TUYA01.
- [32] S. Agostinelli *et al.* (GEANT4 Collaboration), Nucl. Instrum. Meth. A **506**, 250 (2003).
- [33] K. X. Huang, Z. J. Li, Z. Qian, J. Zhu, H. Y. Li, Y. M. Zhang, S. S. Sun, and Z. Y. You, Nucl. Sci. Tech. **33**, 142 (2022), arXiv:2206.10117 [physics.ins-det].
- [34] S. Jadach, B. F. L. Ward, and Z. Was, Phys. Rev. D **63**, 113009 (2001), arXiv:hep-ph/0006359.
- [35] D. J. Lange, Nucl. Instrum. Meth. A **462**, 152 (2001).
- [36] R. G. Ping, Chin. Phys. C **32**, 599 (2008).
- [37] J. C. Chen, G. S. Huang, X. R. Qi, D. H. Zhang, and Y. S. Zhu, Phys. Rev. D **62**, 034003 (2000).
- [38] R. L. Yang, R. G. Ping, and H. Chen, Chin. Phys. Lett. **31**, 061301 (2014).
- [39] E. Richter-Was, Phys. Lett. B **303**, 163 (1993).
- [40] M. Ablikim *et al.* (BESIII Collaboration), Phys. Rev. D **94**, 032001 (2016), arXiv:1512.08627 [hep-ex].
- [41] M. Ablikim *et al.* (BESIII Collaboration), Phys. Rev. Lett. **122**, 062001 (2019), arXiv:1809.06496 [hep-ex].
- [42] M. Ablikim *et al.* (BESIII Collaboration), Phys. Rev. D **95**, 032002 (2017), arXiv:1610.02479 [hep-ex].
- [43] R. M. Baltrusaitis *et al.* (MARK-III Collaboration), Phys. Rev. Lett. **56**, 2140 (1986).
- [44] M. Ablikim *et al.* (BESIII), Phys. Rev. D **109**, 072003 (2024), arXiv:2312.07572 [hep-ex].
- [45] A. Drescher, B. Gräwe, B. Hahn, B. Ingelbach, U. Matthiesen, H. Scheck, J. Spengler, and D. Wegener, Nucl. Instrum. Meth. A **237**, 464 (1985).
- [46] S. M. Flatté, Phys. Lett. B **63**, 224 (1976).
- [47] See Supplemental Material at [URL] for additional analysis information.
- [48] G. S. Adams *et al.* (CLEO Collaboration), Phys. Rev. D **84**, 112009 (2011), arXiv:1109.5843 [hep-ex].
- [49] M. Ablikim *et al.* (BESIII Collaboration), Phys. Rev. D **76**, 122002 (2007).
- [50] W. Wang, Phys. Lett. B **759**, 501 (2016), arXiv:1602.05288 [hep-ph].
- [51] N. N. Achasov, A. V. Kiselev, and G. N. Shestakov, Phys. Rev. D **102**, 016022 (2020), arXiv:2005.06455 [hep-ph].
- [52] D. Becirevic and A. B. Kaidalov, Phys. Lett. B **478**, 417 (2000), arXiv:hep-ph/9904490.
- [53] N. N. Achasov, A. V. Kiselev, and G. N. Shestakov, Phys. Rev. D **104**, 016034 (2021), arXiv:2106.10670 [hep-ph].
- [54] M. Ablikim *et al.* (BESIII), Phys. Rev. D **92**, 072012 (2015), arXiv:1508.07560 [hep-ex].
- [55] H.-Y. Cheng, C.-W. Chiang, and Z.-Q. Zhang, Phys. Rev. D **105**, 033006 (2022), arXiv:2201.00460 [hep-ph].
- [56] M. Ablikim *et al.* (BESIII Collaboration), Chin. Phys. C **44**, 040001 (2020), arXiv:1912.05983 [hep-ex].
- [57] H.-B. Li and X.-R. Lyu, Natl. Sci. Rev. **8**, nwab181 (2021), arXiv:2103.00908 [hep-ex].

**Supplemental Material: Study of the light scalar meson $a_0(980)$ through the decay
 $D^0 \rightarrow a_0(980)^- e^+ \nu_e$ with $a_0(980)^- \rightarrow \eta \pi^-$**
(Dated: November 13, 2024)

Table I summarizes the sources of the systematic uncertainties in the BF measurement of the decay $D^0 \rightarrow a_0(980)^- e^+ \nu_e$ with $a_0(980)^- \rightarrow \eta \pi^-$.

Table II summarizes the covariance matrices with statistical and systematic contributions.

TABLE I. Relative systematic uncertainties in the BF measurement.

Source	Uncertainty (%)
$N_{\text{ST}}^{\text{tot}}$	0.1
π^\pm, e^\pm tracking	0.3
π^\pm, e^\pm PID	0.3
η reconstruction	1.6
$N_{\text{extra}}^{\pi^0}$ requirement	0.7
Lateral moment cut	1.1
Signal model	3.5
Background shape	1.3
U_{miss} resolution	2.9
$\mathcal{B}_{\eta \rightarrow \gamma\gamma}$	0.5
MC sample size	0.1
Total	5.2

TABLE II. Statistical and systematic covariance matrices for the decay $D^0 \rightarrow a_0(980)^- e^+ \nu_e$ with $a_0(980)^- \rightarrow \eta \pi^-$. The total covariance matrix is $C_{ij} = C_{ij}^{\text{stat.}} + C_{ij}^{\text{syst.}}$.

$C_{ij}^{\text{stat.}}$	1	2	3
1	0.000705	-0.000055	0.000002
2	-0.000055	0.000484	-0.000048
3	0.000002	-0.000048	0.000547

$C_{ij}^{\text{syst.}}$	1	2	3
1	0.000032	0.000001	0.000002
2	0.000001	0.000008	-0.000001
3	0.000002	-0.000001	0.000050

C_{ij}	1	2	3
1	0.000737	-0.000054	0.000004
2	-0.000054	0.000492	-0.000049
3	0.000004	-0.000049	0.000597